Macromolecules

Article

pubs.acs.org/Macromolecules

High Molecular Mobility and Viscoelasticity of Microphase-Separated Bottlebrush Diblock Copolymer Melts

Benjamin M. Yavitt,[†] Yue Gai,[†] Dong-Po Song,[†] H. Henning Winter,*[,†,‡] and James J. Watkins*[,†]

[†]Department of Polymer Science and Engineering and [‡]Department of Chemical Engineering, University of Massachusetts Amherst, Amherst, Massachusetts 01003, United States

Supporting Information

ABSTRACT: We investigate the linear viscoelastic behavior of poly(styrene)-*block*-poly(ethylene oxide) (PS-*b*-PEO) AB diblock brush copolymer materials over a range of volume fractions and with side-chain lengths below entanglement molecular weight (PS $M_n \sim 3.5$ kg/mol and PEO $M_n \sim 5$ kg/mol). The high chain mobility of the brush architecture results in rapid microphase segregation of the brush copolymer segments, which occurred after mild thermal annealing. Master curves of the dynamic moduli were obtained by time−temperature superposition (tTS). The reduced degree of chain entanglements leads to a unique liquid-like rheology similar to that of bottlebrush (BB) homopolymers, even in the microphase-segregated state. The microphase-segregated domains were found to align at exceptionally low strain amplitudes ($\gamma = 0.01$) and mild processing temperatures as confirmed by small-angle X-ray scattering (SAXS). Domain/grain orientation occurred readily at strains within the linear viscoelastic regime (LVR) without noticeable effect on the dynamic moduli. This interplay of high molecular mobility and rapid phase segregation contrasts the viscoelasticity of brush block copolymers (BBCP) compared to conventional linear block copolymer (LBCP) analogues and opens up new processing possibilities of BBCP materials for a wide range of nanotechnology applications.

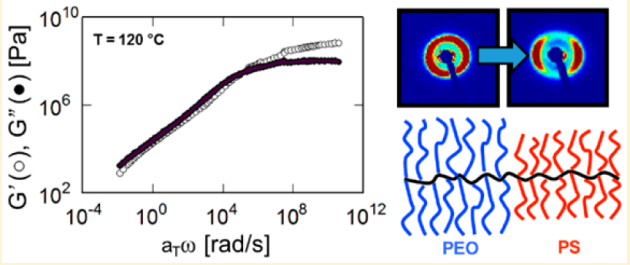

INTRODUCTION

Brush or bottlebrush (BB) macromolecules have attracted increased attention due to their unique physical properties. Designed to mimic the "bottlebrush" architecture, the macromolecules have side chains grafted along the entire polymeric backbone. Precise synthetic approaches have resulted in polymers with side chains uniform in length at very high grafting density (essentially one side chain per monomer in the backbone).[1] Because of the low degree of polymerization within side chains and steric repulsion arising from dense grafting densities, BB polymers may remain unentangled in the melt up to unusually high molecular weights, and the molecular mobility remains high.[2]

Side chain chemistry, side chain length, and backbone length strongly affect the BB rheology as seen in small amplitude oscillatory shear (SAOS) and creep experiments.[3−7] The full dynamic modulus response highlights the relaxation patterns of each component of the BB design, from the side chains to the molecular backbone. In macromolecules with short side chain length, the formation of an entanglement plateau is completely absent. Dynamic moduli $G'(\omega)$ and $G''(\omega)$, over a wide frequency range, transition directly from liquid behavior at low frequencies to glassy behavior at the highest frequencies. As side chain length increases, an entanglement plateau begins to emerge in the fast relaxation regime, corresponding to the relaxation of those tethered side chains.[3,5] The size of the linear polymeric backbone determines the longer relaxation times, which governs behavior at lower frequencies and long-time exposures to stress and strain. In this regime, backbones behave as unentangled chains and the relaxation process and can be described by classical Gaussian chain dynamics theory. Both Rouse-like and Zimm-like scaling behaviors have been observed.[5] Only at exceptionally large backbone length, an additional entanglement plateau begins to emerge leading to "double relaxation" behavior.[3] In the low frequency limit, the BBs still retain liquid behavior with power law scaling $G'(\omega) \sim \omega^2$ and $G''(\omega) \sim \omega$.

The high molecular mobility of the BB molecules provides an opportunity to design a new class of copolymer materials with fast microphase segregation, known as brush block copolymers (BBCP). AB diblock brush copolymers (referred to throughout as dbBB, or "diblock bottlebrushes") are macromolecules with two sections, each having their own type of polymeric side chains densely grafted to the molecule's backbone.[8,9] Highly extended backbone conformations and significant repulsion between grafted side chains are believed to suppress chain entanglements.[8−11] As a result, dbBBs rapidly self-assemble into a range of ordered morphologies with periodicity up to and above 100 nm. dbBBs have already shown potential in applications such as directing large nanoparticle arrays,

Received: July 8, 2016
Revised: October 5, 2016
Published: December 23, 2016

DOI: 10.1021/acs.macromol.6b01471
Macromolecules 2017, 50, 396−405

photonic crystals, and porous materials.[12−17] Liquid crystalline side chains may also be grafted to the molecular backbone acting as one of the blocks. This has led to unique self-assembly behavior, directed domain alignment, and many more potential applications.[18,19]

The fast dynamics of the BBCPs is in contrast to the slow ordering dynamics of the linear block copolymers (LBCP), which are able to self-assemble into structures with periodicity from a few to several tens of nanometers when given enough time.[20−22] The ordering dynamics of LBCP demands for higher annealing temperatures and longer annealing times which limits their applicability at the industrial scale.

Shear deformation has been found to induce structural alignment in LBCPs.[23−25] Controlled oscillatory shear and steady shear typically direct domain orientation in LBCP templates systems such as PS-*b*-PI, PS-*b*-PB, PS-*b*-PB-*b*-PS, and PEP-*b*-PEE.[26−31] Traditionally, LBCP materials have been aligned through nonlinear shear deformations (on the order of $\gamma = 0.1-1$) at elevated processing temperatures often near the order-to-disorder transition temperature (T_{ODT}). However, lower operating temperatures are more desirable for large-scale processing and imprinting techniques. Additionally, orientation effects at low strain amplitudes within the linear viscoelastic regime (LVR) have not been reported as far as we know. In the view of these limitations for LBCP, the high mobility of BBCPs and their rapid self-assembly lead to interesting opportunities in controlling the orientation of the structure.

To our knowledge, there are no reports on the dynamics of neat dbBB systems with high grafting density and short side chain lengths. A few studies have been conducted on various comb-like/graft copolymer systems, but with much lower grafting densities (less than one side chain/backbone monomer) than the architectures of interest (maximum grafting density of one side chain/backbone monomer).[32−37] Most recently, dynamic mechanical analysis was conducted on PS-*b*-PEO-*b*-PS ABA triblock brush copolymer (tbBB) ion gel materials by Bates et al., yet the full dynamic response was not presented in detail.[38,39] A comprehensive understanding of relaxation and flow properties through rheological characterization is crucial for describing the molecular mobility of dbBBs and for the future implementation of these materials in an industrial setting, such as flow coating or roll-to-roll processing.

In this work, we explore the linear viscoelasticity and molecular dynamics of characteristic dbBBs in the microphase-segregated melt state. We specifically study the dynamic mechanical response over a wide frequency range as well as demonstrate the onset of orientation in BCP domains at small strain amplitudes. Overall, these BBCP materials combine the molecular architecture of the BB homopolymers with the heterogeneous phase segregation behavior of the LBCP, each distinctly contributing to the viscoelastic behavior. By combining both dynamics into one molecular design, new dynamics and a new structure−property relationship emerge.

EXPERIMENTAL SECTION

Materials. A series of well-defined AB diblock poly(styrene)-*block*-poly(ethylene oxide) (PS-*b*-PEO) dbBBs (side chain length PS $M_n \sim 3.5$ kg/mol and PEO $M_n \sim 5$ kg/mol) as a function of PEO volume fraction ($f_{PEO} = 0.24$, 0.49, and 0.81) (see Table 1) were synthesized by sequential ring-opening metathesis polymerization (ROMP) according to established procedures (see Supporting Information for synthesis characterization).[14−17,40] The side chain lengths were kept constant at molecular weights below the entanglement molecular weight in order to take full advantage of the fast ordering dynamics as observed for such polymers in previous studies.[14−17] Linear AB diblock PS-*b*-PEO were purchased from Polymer Source. Inc. with the purpose of comparing the ordering dynamics and viscoelasticity of dbBBs with that of conventional diblock linear architectures (referred to throughout as "dbLin") across similar volume fraction ($f_{PEO} = 0.22$, 0.47, and 0.81)

Table 1. Characteristics of PS-*b*-PEO Bottlebrush and Linear Diblock Copolymers

PS-*b*-PEO sample name[a]	M_w[b] (kg/mol)	f_{PEO}[c] (vol %)	M_w/M_n[b]	*d*-spacing[d] (nm)
dbBB-24	714.4	24	1.28	42.5
dbBB-49	473.6	49	1.09	57.3
dbBB-81	401.9	81	1.16	32.5
dbLin-22	49	22	1.06	33.8
dbLin-47	76	47	1.08	66.5
dbLin-81	88.4	81	1.08	44.9

[a]Sample names are labeled in the following convention: *X*-*YY*, where *X* is either "dbBB" or "dbLin" to denote bottlebrush or linear architecture respectively, and *YY* signifies the percentage of PEO domain volume fraction. [b]M_w of dbBBs were determined by GPC MALLS. [c]f_{PEO} of dbBBs were calculated using ^{1}H NMR spectra as well as bulk densities $\rho_{(PEO)} = 1.08$ g/cm^3 and $\rho_{(PS)} = 1.05$ g/cm^3. [d]Domain spacing was calculated using $d = 2\pi/q^*$, where q^* corresponds to the primary scattering peak in SAXS. Material characteristics of dbLin were provided by the supplier.

Sample Preparation. A 2 wt % solution of dbBB was prepared in anhydrous dichloromethane (DCM) and drop-cast onto glass under a nitrogen atmosphere on a flat stage. After the solvent was evaporated, the dried films were collected. dbLin materials were used as received. Approximately 30 mg of bulk material was packed into a circular metal mold and sandwiched between pieces of Kapton tape. The samples were annealed under vacuum for 1 h at 110 °C (dbBB) or 24 h at 120 °C (dbLin). The samples were subsequently cooled to room temperature.

Experiments. Microphase segregation, domain spacing, and domain orientation of the materials were characterized using small-angle X-ray scattering (SAXS) using a Ganesha SAXS-LAB instrument with Cu Kα 0.154 nm line on SAXS or ESAXS mode. Domain spacings $d = 2\pi/q^*$ were determined from q^* = primary peak position. Dynamic moduli between $\omega = 1$ and $\omega = 100$ rad/s were measured by small-amplitude oscillatory shear (SAOS) using a Malvern Kinexus rotational rheometer and an 8 mm parallel plate geometry. Measurements were conducted within the linear viscoelastic regime (LVR) at strain amplitudes of $\gamma = 0.01$ for dbBB and $\gamma = 0.005$ for dbLin materials confirmed by strain amplitude sweeps at $\omega = 1$ rad/s from $\gamma = 0.001$ to $\gamma = 1$ at constant temperature $T = 110$ °C. SAOS isothermal frequency sweeps in 10 K intervals were performed from 150 °C to the PEO melting point T_m (60 °C), avoiding disruption from crystallization. dbLin experiments ranged from 170 to 110 °C, below which the glass transition (T_g) of PS began to interfere with rheological measurements.[26] The time−temperature superposition (tTS) principle was found to apply over a wide temperature range, but not for all compositions. Rheological data were analyzed using IRIS Rheo-Hub 2014 software.[41]

Separate samples were prepared and characterized by SAXS before and after shearing in the parallel plate geometry. 2D SAXS patterns were collected at locations along the radial direction on the circular sample from the center ($r = 0$) to the outer edge ($r \approx R = 4$ mm). The samples were then subjected to single frequency oscillatory time sweeps at constant frequency ($\omega = 1$ rad/s), constant strain amplitude ($\gamma = 0.01$), and constant temperature ($T = 110$ °C) for extended periods of time ($t = 2$ h). After cooling down to room temperature, the samples were again scanned by SAXS at positions along the radial direction as well as 8 points equally distributed azimuthally (every $\theta_{azimuthal} = 45°$) near the edge of the disk-shaped sample.

DOI: 10.1021/acs.macromol.6b01471
Macromolecules 2017, 50, 396−405

RESULTS

Phase Segregation and Structure Characterization. The dbBB materials microphase segregated very quickly, as expected from previous studies. After thermal annealing for just 1 h at 110 °C, dbBBs had strongly phase segregated as indicated by a primary peak in 1D SAXS spectra (Figure 2a) at domain spacings of 42.5, 57.3, and 32.5 nm for dbBB-24, dbBB-49, and dbBB-81 respectively. For asymmetric architectures at high f_{PEO} at low temperature, additional scattering around q = 0.4 nm^{-1} emerged due to presence of PEO crystalline lamellae.

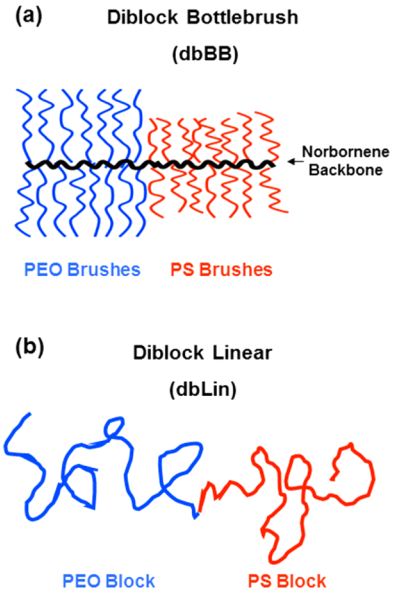

Figure 1. Schematic of poly(styrene)-*block*-poly(ethylene) (PS-*b*-PEO): (a) bottlebrush diblock copolymers (dbBB) and (b) linear diblock copolymer (dbLin) architectures at $f_{PEO} \sim 0.5$.

This was confirmed by heating above the melting temperature of PEO (~65 °C) in temperature-controlled SAXS for two samples dbBB-49 and dbBB-81, at which point the peaks began to disappear (Figures 2b and 2c, respectively). The scattering from the PEO crystals extends over the expected q range of higher order scattering peaks from the phase-segregated structure. In order to determine the morphology, dbBB-49 and dbBB-81 were heated well above 65 °C, at which point weak higher order peaks were resolved. The specific morphology behavior of PS-*b*-PEO dbBBs is a topic of current research and has recently been described by Gai et al.[40] The asymmetry of the volume fraction has a significant effect on the morphology. At the lowest f_{PEO} (dbBB-24), a "wormlike" morphology is observed, consisting of a PEO minor phase in a PS matrix. This was apparent from SAXS (Figure 2a), in which strong phase segregation was observed from the primary peak, but the absence of a second-order peak indicates weak periodicity and long-range order of the microphase-segregated structure. Scattering from PEO crystals was not apparent in this sample due to the low vol % of PEO, and therefore it was not necessary to heat the material above the "melting" temperature. Additionally, at symmetric f_{PEO} (dbBB-49), lamellar morphology arises, and at the highest asymmetry (dbBB-81), cylindrical morphology consisting of PS cylinders in a PEO matrix is present. These characterizations are additionally supported by transmission electron microscopy (TEM) analysis of cryo-microtomed samples (Supporting Information Figure S3).

Dynamic Moduli Response. The full dynamic response of the dbBB architecture was analyzed for tTS behavior (Figure 3). Master curves with $f_{PEO} \sim 25\%$ and $f_{PEO} \sim 50\%$ were shifted to a reference temperature of T_{ref} = 120 °C. This T_{ref} was chosen because it was within the experimental temperature range of all samples and slightly above the approximate T_g of neat PS. Shift factors a_T (Figure 3b) show good fit to the Williams–Landel–Ferry (WLF) equation, indicating realistic temperature dependence of the dynamic response. Vertical shift factors b_T were found to be close to 1 (no vertical shifting required). The ability to apply tTS at temperatures as low as 60 °C for the dbBBs is consistent with the reduced T_g of the PS domain, which contains PS side chains of low molecular weight when compared to the dbLin samples. It is known that T_g generally decreases with decreasing molecular weight. In addition to being tethered at one end, the short PS side chains (3.5 kg/mol) should exhibit reduced T_g. The absence of an inflection point in DSC measurements (Figure S4) of low and high f_{PEO} dbBBs between PEO melting at ~60 and 110 °C

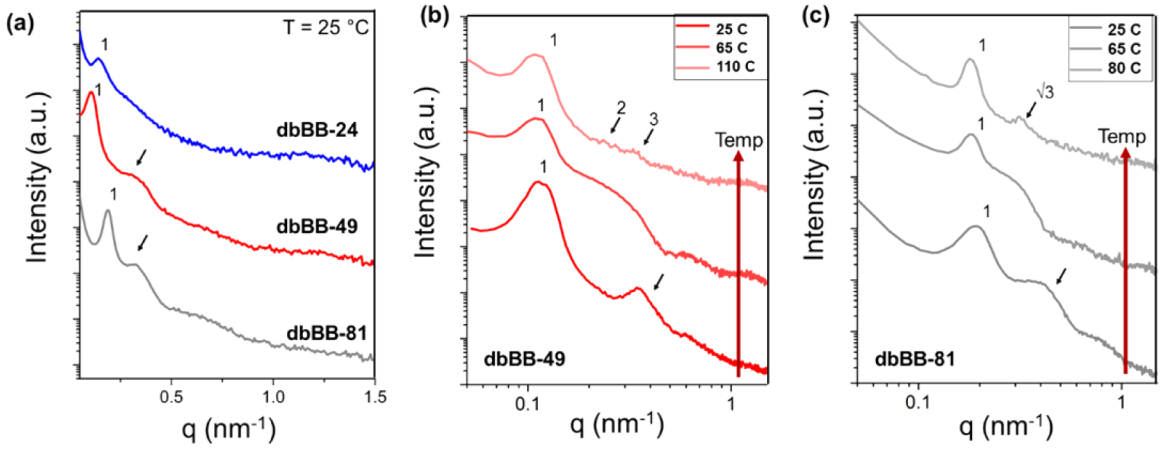

Figure 2. (a) 1D SAXS spectra of dbBB materials after thermal annealing. "1" indicates primary peak. Arrow indicates scattering from PEO crystals. (b) Temperature-controlled SAXS of dbBB-49 upon heating from room temperature to 65 and 110 °C. After heating the scattering signal from PEO lamellae disappears. At 110 °C, weak second- and third-order peaks are resolved at peak ratios $q^*:q_2:q_3$ = 1:2:3 indicating lamellar morphology. (c) Temperature-controlled SAXS of dbBB-81 upon heating from room temperature to 65 and 80 °C. After heating the scattering signal from PEO lamellae disappears. At 80 °C a higher order peak may be resolved at peak ratio $q^*:q_2 = 1:\sqrt{3}$ indicating cylindrical morphology.

DOI: 10.1021/acs.macromol.6b01471
Macromolecules 2017, 50, 396–405

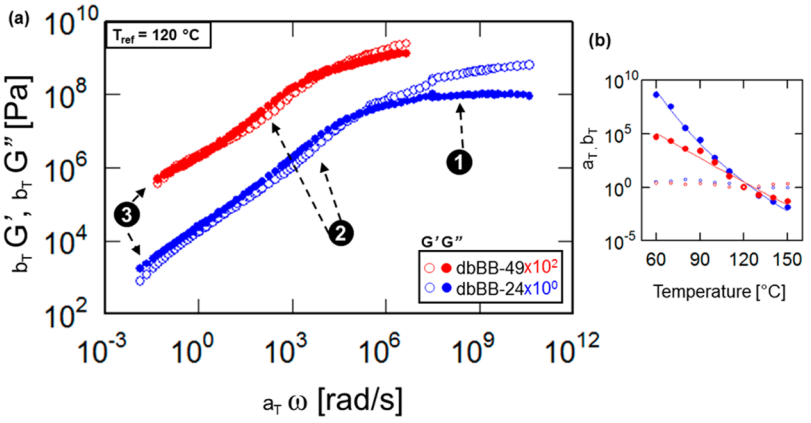

Figure 3. (a) Master curves of dynamic moduli $G'(\omega)$ (open symbols) and $G''(\omega)$ (closed symbols) for PS-*b*-PEO dbBB samples at a reference temperature of T_{ref} = 120 °C. Labels indicate the following features: (1) glassy region, (2) intermediate relaxation, (3) confined terminal flow. dbBB-49 master curve shifted vertically by additional indicated scaling factor to provide clarity. (b) Time−temperature superposition shift factors a_T (closed symbols) and b_T (open symbols) for master curves. Line shows fit to the WLF equation.[42]

confirms this behavior. Therefore, it is reasonable to achieve rheological measurements and apply tTS to much lower temperatures while remaining in the melt state. Ideally, the master curves encompass the entire relaxation response, from terminal flow to glassy behavior. At the shortest relaxation times above frequencies $a_T\omega = 10^4$−10^5 rad/s, glassy behavior (here indicated by $G'(\omega) > G''(\omega)$) is well-defined rheologically for dbBB (Labeled as region 1).

At frequencies below $a_T\omega = 10^4$ rad/s, $G''(\omega)$ dominates and the materials begin to behave mostly viscous. We noticed that the dynamic response of the dbBB was primarily viscous over the entire remaining intermediate frequency range (region 2) below the glassy region. There is no distinct rubbery plateau, as would be expected in entangled LBCP systems (Figure S5). The terminal flow regime (region 3) is that of a liquid but does not reach the classical limiting behavior (slopes of 2 and 1 for $G'(\omega)$ and $G''(\omega)$, respectively) even at the lowest temperatures. Because of instrument and sample limitations, we were unable to obtain additional data in the low frequency regime and apply power law scaling to the dynamic modulus' frequency dependence.

The rheological characterization of the $f_{PEO} \sim 80\%$ samples (both dbBB-81 and dbLin-81) yielded data that could not be shifted using tTS. These materials were found to be inherently thermorheologically complex (elaborated in the Discussion section). dbBB-81 simply behaved as a soft solid over the experimental temperature range. For PS-*b*-PEO BCPs, as f_{PEO} increases, thermorheological simplicity breaks down. At this point, the origin of the thermorheological complexity in the high f_{PEO} sample is unclear. It is important to point out that this is not the first occurrence of this type of behavior. The dynamic moduli of PS-*b*-PEO-*b*-PEO triblock brush block copolymers (tbBBs) with high volume fraction PEO (f_{PEO} = 0.75) over a temperature range of 40−105 °C showed similar soft solid behavior as well as failure of tTS.[39]

After rheological characterization, all of the samples were cooled down to 25 °C and removed from the rheometer for SAXS to determine any changes in phase segregation (Figure S6). The primary peaks in 1D SAXS remained the same, and there were minimal changes in domain spacing, indicating that phase segregation was maintained throughout the rheological characterization.

Strain Amplitude Response. A range of linear viscoelastic behavior was investigated in order to establish shear strain effects on the modulus response before conducting shear alignment studies. Samples of symmetric $f_{PEO} \sim 50\%$ (dbBB-49 and dbLin-47) were subjected to increasing strain amplitude at constant frequency (ω = 1 rad/s) and temperature (T = 110 °C).

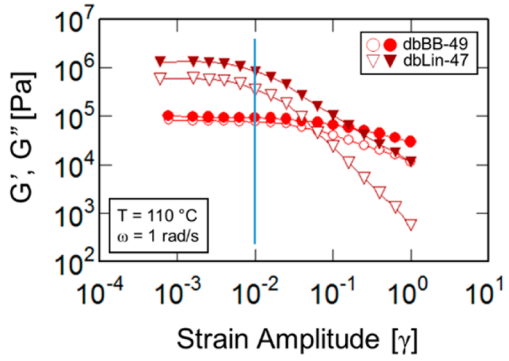

Figure 4. Variation in storage modulus G' (open symbols) and loss modulus G'' (closed symbols) at increasing strain amplitude for dbBB-49 and dbLin-47. Strain of 1% (γ = 0.01) is highlighted by a vertical line.

Within the LVR, the dynamic moduli response appears to be independent of applied strain. As the strain amplitude increases, G' and G'' begin to deviate and decrease, leading to a regime of nonlinear dynamic modulus response. The dbLin-47 response is plotted along with dbBB-49 to provide a comparison. At the selected frequency and temperature, it is apparent that the LVR of the dbBBs persists to much higher strains than the dbLins. The steep drop-off observed in dbLin-47 is also noted. G' and G'' drop an order of magnitude more than for dbBB-49 after increasing strain amplitude to γ = 1 (or 100%).

Shear-Induced Domain Orientation. The structure−property relationship of the dbBBs was further investigated with regards to domain and grain orientation as well as sample homogeneity. 2D SAXS patterns of separately prepared dbBB-49 and dbLin-47 were collected along the radial axis of thermally annealed samples. After thermal annealing, there was no apparent preferred orientation of the phase-segregated

DOI: 10.1021/acs.macromol.6b01471
Macromolecules 2017, 50, 396−405

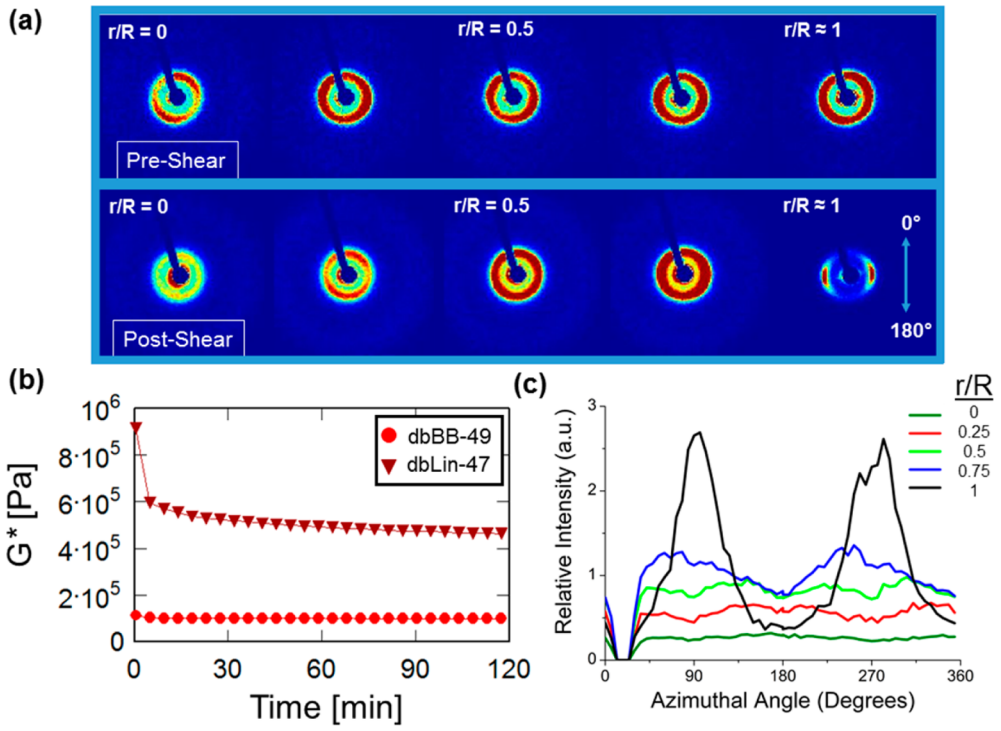

Figure 5. (a) 2D SAXS patterns along radial axis of dbBB-49 before and after single frequency time sweeps. (b) Complex modulus G^* variation during time sweeps for dbBB-49 and dbLin-47. (c) Relative Intensity of primary peak vs azimuthal angle at various radial position (r/R) of dbBB-49 after shearing. Larger r/R corresponds to larger applied shear amplitude (where $r/R \approx 1$ corresponds to $\gamma = 0.01$).

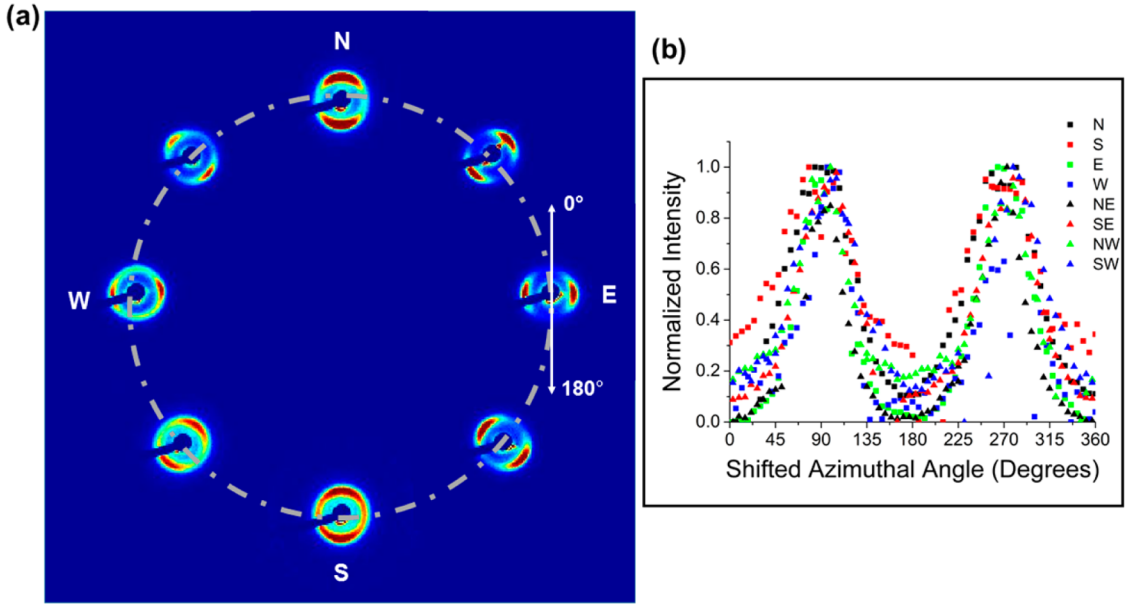

Figure 6. (a) 2D SAXS patterns around sample edge ($r/R \approx 1$) of dbBB-49 after single frequency time sweeps. (b) Normalized intensity of primary peak vs shifted azimuthal angle for corresponding 2D SAXS patterns. 0° and 180° correspond to direction of applied shear.

domains in dbBB-49 (Figure 5a). At most points along the radial axis from the center of the sample ($r = 0$) to the edge ($r \approx R$), a powder diffraction pattern for the primary peak was observed.

The samples were then subjected to single frequency oscillatory time sweeps ($\omega = 1$ rad/s) for 2 h at a strain amplitude of $\gamma = 0.01$ and constant temperature $T = 110$ °C. This strain was previously determined to be within a LVR of dbBB-49, but slightly into the nonlinear regime of dbLin-47. This is highlighted in Figure 5b, where the dbLin-47 complex modulus initially drops significantly under the applied deformation, while the dbBB-49 complex modulus stays constant during the entire processing time. This characteristic LBCP behavior has been previously reported in other shear alignment studies.[29]

After shearing, the samples were scanned again along the radial axis. No changes in the dynamic modulus response of dbBB-49 were observed during shearing, yet after shearing we

DOI: 10.1021/acs.macromol.6b01471
Macromolecules 2017, 50, 396−405

observed a very distinct transition in the preferred orientation of the BCP domains. At the center of the sample, a powder diffraction pattern was still present, and no preferred orientation was observed in the Intensity of primary scattering peak vs azimuthal angle plot of the 2D SAXS pattern. At radial locations closer to the edge, the intensity of the first-order peak began to increase as well as the preferred azimuthal angle. At the very outer edge, strong scattering signal arising from domain alignment was observed as shown in the 2D SAXS pattern.

Figure 5c shows primary peak intensity dependence on azimuthal angle at increasing radial distance from the center. As the applied strain amplitude increased with increased distance from the center, a preferred orientation begins to emerge. At r/R = 0.75, the beginning of a preferred azimuthal angle dependence appears and becomes very strong at $r/R \approx 1$. The observed 2D SAXS pattern indicated that the phase-segregated domains are aligned with the vorticity plane of the shear. This would suggest the perpendicular orientation for lamellar morphology.[23,24,28] No apparent changes in domain orientation were observed in dbLin-47 at the same shearing conditions (Figure S7).

Corresponding 1D SAXS indicate that the microphase segregation was unchanged during the application of shear. Spectra at $r/R \approx 1$ show no changes in phase segregation strength or domain spacing (Figure S8). Additionally, the microphase separation persists at the shearing temperature as shown with temperature-controlled SAXS (Figure 2b). The anisotropy in the 2D patterns most likely arises simply from grain rotation rather than a morphology or structural transition. These experiments were performed outside the rheometer. To understand and observe the transient structures of dbBBs under different shearing states, in-situ SAXS/shearing measurements are planned.

Additionally, 2D SAXS patterns were collected at points along the outer edge ($r/R \approx 1$) where anisotropy was the strongest (Figure 6a). The preferred domain direction correlates very well to the applied shear direction. Normalized intensities of the primary peak were shifted according to the applied oscillatory shear direction (corresponding to $\theta_{azimuthal}$ = 0° and 180°) at each location on the outer edge (Figure 6b). At all points around the edges, the primary peaks align perpendicular (at 90° and 270°) to the applied shear direction.

DISCUSSION AND DATA ANALYSIS

Overall, the dbBBs seem to exhibit a unique structure−property relationship between the phase segregation and viscoelasticity. It is clear that the dbBBs self-assemble into strongly phase segregated domains and structures. It is also important to note the unusually fast ordering dynamics and high mobility in the dbBB systems despite their high molecular weights. In order to compare the rheological response of dbBB and dbLin samples with similar phase segregation and domain spacing, it was necessary to anneal the dbLin for longer times (24 h) at higher temperatures (120 °C). For comparison, separate dbLin samples were annealed at identical conditions to the dbBB (1 h at 110 °C). 1D SAXS showed no strong scattering peaks (Figure 7a). Longer annealing periods were required to achieve adequate spacings and phase segregation strength in the dbLin, resulting in domain spacings of 32.6, 66.5, and 44.8 nm for dbLin-22, dbLin-47, and dbLin-81, respectively (Figure 7b). The reduced degree of chain entanglements in BBCPs increases chain mobility while strong differences between blocks

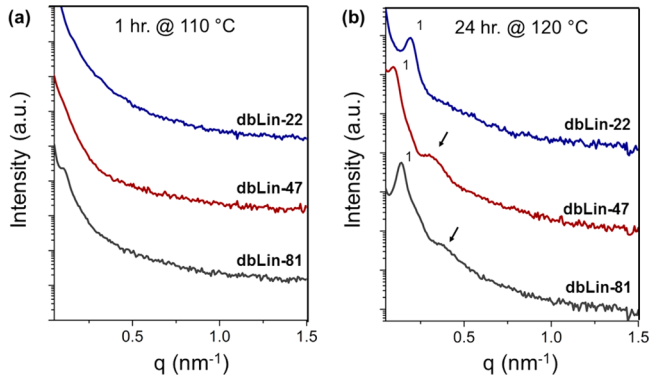

Figure 7. (a) SAXS spectra of dbLin after 1 h thermal annealing at 110 °C. Note the poor phase segregation. (b) SAXS spectra of dbLin after 24 h thermal annealing at 120 °C, which formed microphase-segregated structures and were used for rheological characterization.

(resulting in large Flory−Huggins parameter (χ)) still provides a driving force for phase segregation. This in turn required milder thermal annealing conditions.

The dbBB viscoelastic response depicted in the master curve (Figure 3a) is remarkably similar to that of the BB homopolymers, specifically their liquid-like nature and lack of entanglement plateau. In the melt state, both dbBB-24 and dbBB-49 proceed directly from primarily viscous behavior at low frequency to glassy behavior at high frequency ($a_T\omega = 10^4$ rad/s), much like BB homopolymer materials with short side chains.[5,6] Even within the phase-segregated domains, the bottlebrush side chains provide a relatively liquid-like environment for the relaxation of the main backbone chains. Additional analysis of the data further highlights this unique behavior. For example, the Booij−Palmen plot is a useful tool for investigating the rheological behavior of bulk polymeric materials as well as confirming the applicability (or lack of applicability) of tTS.[43−45] Booij−Palmen plots were constructed for the dbBB series (Figure 8a) and the dbLin (Figure 8b). In this plot of normalized phase angle ($2\delta/\pi$) vs complex modulus (G^*), tTS can be applied if the individual frequency sweeps at each temperature collapse onto a single curve. The dbBB samples display thermorheological simplicity over the experimental temperature range. As previously mentioned, the exception is dbBB-81, which does not obey tTS as indicated by the lack of superposition of the $\delta(G^*)$ curves.

The applicability of tTS to heterogeneous materials, such as phase-separated block copolymers, seems counterintuitive. It is generally considered that tTS will hold when the various relaxation times of a relaxation process have the same temperature dependence.[43,44] One would think that a system with many components would inherently fail tTS, in the sense that multiple relaxation processes maintain individual temperature dependence. Palmen tested the applicability of tTS on various polymer blends, both miscible and immiscible.[43,44] Some of the blends would fail tTS while others would hold. Additional accounts suggest that there is no theoretical basis for this to occur.[46] Possible explanations highlighted by Palmen suggest that if the activation energies or WLF parameters of the components are similar, then tTS may hold. Additionally, the failure of tTS can be subtle and not picked up through experimental methods, especially in asymmetric systems with a small volume fraction of one component.[43] Considering the asymmetry in our phase-separated block copolymer system, it is possible that the major phase is dominating the relaxation

DOI: 10.1021/acs.macromol.6b01471
Macromolecules 2017, 50, 396−405

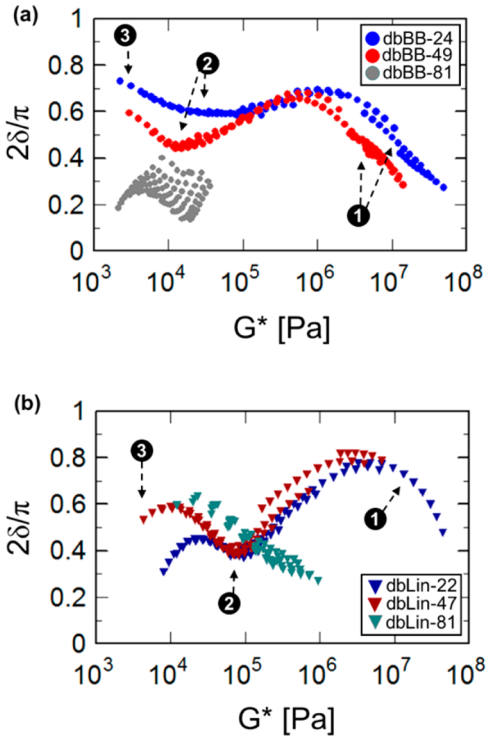

Figure 8. Booij–Palmen plot of (a) BBCP materials dbBB-24, dbBB-49, and dbBB-81 and (b) LBCP samples dbLin-22, dbLin-47, and dbLin-81. Labels correspond to features presented in Figure 3. tTS cannot be applied to samples with $f_{PEO} \sim 80\%$. The frequency sweep data do not overlap, highlighting the thermorheological complexity of the material.

response. Above its T_g, PS-rich materials generally display thermorheologically simple behavior.[27] On the other hand, there are few accounts of tTS for PEO-rich materials in the molten state. This may explain the emergence of thermorheological complexity in dbBB-81.

Furthermore, in Figure 8a, at larger G^* values above 10^7 Pa (corresponding to the lowest testing temperatures), discontinuities in the overlapping of the curves begin to emerge. This behavior is characteristic of materials passing through a glass transition, and it is very apparent in the Booij–Palmen plot. Relaxation processes are indicated by local minima in $\delta(G^*)$.[5,43,47] In both dbLin samples, strong minima occur at $G^* \sim 10^5$ Pa associated with the chain entanglement plateau, whereas dbBB-24 and dbBB-49 show drastically reduced minima (region 2). In the case of dbBB-24, the minimum is very broad and at large phase angle, indicating primarily viscous behavior. For dbBB-49, the minimum is more apparent, but reduced by an order of magnitude in modulus ($G^* \sim 10^4$ Pa) compared to dbLins. This is most likely a relaxation of the molecular backbone, rather than the side chains, which would be expected at higher G^* values.[3,5] At the lowest modulus values (below 10^4 Pa), the liquid-like behavior of the BBCP is very apparent, as the curves for dbBB-24 and dbBB-49 curve upward to higher phase angle. Comparatively, dbLin-22 and dbLin-47 immediately begin to slope toward smaller phase angle and more elastic, solid-like character.

The complex viscosity (η^*) response over the range of complex modulus (G^*) values was plotted using data from the master curves (Figure 9a). The power law scaling in this plot describes the liquid–solid characteristic, in which small negative slopes correspond to liquid-like behavior and larger negative slopes correspond to solid-like behavior.[51] At large G^* values, the dbBBs shows solid-like glassy behavior. The dbLin samples show the onset of the glassy behavior, but as previously stated the full response did not shift onto the master curve. At $G^* \sim 10^5$ Pa, the rubbery plateau of the dbLin becomes pronounced, as indicated by a drastic change in slope ($\eta^* \sim G^{*-1.5}$). The slopes for each dbBB sample follow less steep power law trends (−0.75 and −1.2 for dbBB-24 and dbBB-49, respectively), indicating more liquid-like behavior throughout the same regime. The slight hump in dbBB-49 at $G^* \sim 10^4$ Pa corresponds to the possible relaxation of the backbone as observed in the Booij–Palmen plots. Additionally, it should be noted that the dbBBs exhibit a much lower η^* at respective G^* values, indicating higher inherent mobility and possibly more desirable processability overall.

At the lowest frequencies, it is very surprising that viscous behavior continues to exist. To further investigate this, we calculated relaxation time spectrum (Figure 9b) from the master curve dynamic data in Figure 3 according to Baumgaertel et al.[48] Overall, the dbBB materials show a distribution of inherently shorter relaxation times, an indication of the high molecular mobility. Interestingly, the spectra essentially superimpose upon one another. dbLin-22 and

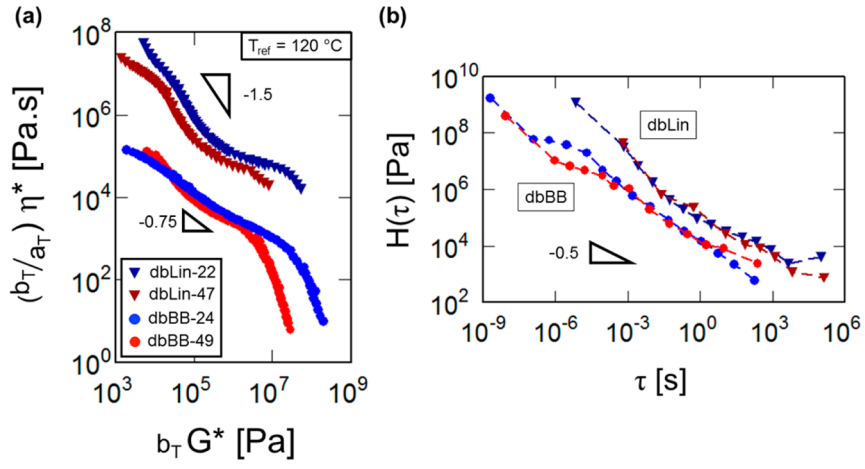

Figure 9. (a) Winter plot (η^* vs G^*) of dbLin and dbBB at T_{ref} = 120 °C using master curve data.[51] (b) Relaxation time spectrum calculated from master curves at T_{ref} = 120 °C. Spectra calculated according to Baumgaertel et al.[48]

DOI: 10.1021/acs.macromol.6b01471
Macromolecules 2017, 50, 396–405

dbLin-47 exhibit longer characteristic times and are also indistinguishable from one another. In this case there is a clear categorization of the two architectures into different regimes of characteristic relaxation time distributions. Several decades of power law scaling were observed ($\tau = 10^{-3}$ to $\tau = 10^{3}$) and dbBB and dbLin spectra fit roughly to a slope of −0.5 in that regime. The long time behavior is directly related to the low frequency response in the master curve. dbLin-22 and dbLin-47 begin to show some additional long time modes, indicated by the slight plateau at the end of the spectra. This trend was not fully resolvable in the master curve data but is more apparent in the relaxation spectrum. The microphase segregation of the BBCP has very little effect on the dynamics in this regime. This behavior is significantly different from that of the conventional LBCP, for which elasticity often persists at the lowest frequencies. The qualitative and quantitative behavior of elasticity is often directly related to the degree of phase segregation and the morphology.[49] We attribute the absence of elastic behavior to the inherently fast dynamics and mobile behavior of the brush architecture. In this low frequency regime, the response of the nanostructure dominates the viscoelastic response, yet the chains still have the freedom to rearrange and relax within the domains. This can only be said about the thermorheologically simple samples (dbBB-24 and dbBB-49) as their low frequency response is observable through the application of tTS. The fact that dbBB-81 remains solid-like (as indicated in Figure 8a) is still surprising. Overall, the liquid-like behavior of these select BBCP is supported quantitatively despite strong microphase segregation and is consistent with the fast ordering dynamics that are a consequence of reduced chain entanglements.

Prior investigations of BB homopolymer systems have shown that the lengths of the side chains and backbone dictate the magnitude of the various relaxation features observed over the frequency range.[3] For example, the longest relaxation process becomes more predominant with increasing backbone length.[5] The corresponding modulus value (identified by the minima in the Booij−Palmen plot) is then an indication of the overall molecular mass of the molecule ($G^* \approx \rho RT/M_w$, where ρ, R, T, and M_w are density, gas constant, temperature, and overall molecular weight, respectively).[47] A BBCP contains two competing chemical structures and side chain lengths, which presumably affect the backbones rigidity differently. Therefore, it is apparent that there are several parameters (volume fraction, block length, overall length, etc.) that must be dissociated in order to quantify the true contribution of the molecular backbone to the observed rheological response. In our material series, volume fraction, overall MW, and overall density are all changing from sample to sample. At this time we cannot make a precise conclusion on the backbone relaxation correlation. To fully investigate volume fraction effects as well as possible morphology effects in relation to backbone length, a new more extensive series of samples with constant backbone length and varying volume fraction must be synthesized and characterized. We hypothesize that the trends will closely mirror trends from previous BB homopolymer investigations.

Remarkably, the orientation of the phase-segregated domains in the dbBB also has little effect on the viscoelastic response. This behavior was completely unexpected. Traditionally, shear-induced domain orientation is produced by nonlinear shear deformations. These high shear strains are necessary to overcome the thermodynamic barriers associated with local destructions and re-formations (i.e., mixing) of the phase-segregated domains and to remove grain boundaries.[26−29,50] This is coupled with a softening of the material with time. In the dbBB, the onset of this behavior is observed in an entirely new regime of SAOS, where we assume the applied shear does not perturb the structure. The existence of the grain boundaries does not affect the rheology, so removal by shear alignment is not noticeable by rheological experiments. Modulus values remained invariant with time during oscillatory shear. The transition is only detectable through structural characterization using SAXS. This disconnect in the structure−property relationship is unusual and has not yet been reported in BCP materials to our knowledge. The mechanism of alignment, whether it be grain rotation or destruction/re-formation, is also unclear at this time and will garner attention in future studies. Specifically with dbBB-49, the scattering pattern indicates a possible perpendicular alignment of the domains. Traditionally in lamellar morphologies, the domains align in parallel, perpendicular, or transverse orientations and are a function of the applied strain and frequency.[23,24] Parallel orientations are most stable and most common, so the appearance of perpendicular orientation is surprising. It has been well established that the production of oriented structure with LAOS is closely coupled to the dynamics of the dbLin polymer. As dbBBs exhibit much faster, mobile molecular dynamics than their dbLin counterparts, it can be expected that the dynamics may affect any orientation in a completely new way. In our investigation, only one shearing condition was examined. This first observation is striking and opens a new opportunity to correlate the molecular dynamics of dbBBs to the behavior of materials on the bulk scale.

The demonstration of shear-induced ordering in these dbBB materials is very interesting and especially appealing for implementation in future processing applications. As previously stated, the controlled domain ordering at small strain amplitude (within the LVR) and at low temperature ($T_g < T \ll T_{ODT}$) is unique to the BBCP architecture. This provides an entirely new regime of potential processing conditions for the controlled assembly of BBCP domains via shear deformation. Advantages of reducing the processing temperature include speeding up processing time, reduced energy use, and reducing the chance of sample degradation. These highlights all convey the potential for BBCP implementation in applications where nanoscale domain alignment must be easily and efficiently controlled.

CONCLUSION

In summary, we investigated the linear viscoelastic behavior of a robust PS-*b*-PEO diblock brush copolymer system with side chains below entanglement molecular weight. Their unique rheological behavior was compared to that of linear block copolymer analogues. The viscoelastic response of the dbBB was highlighted by the absence of a side chain entanglement plateau in the master curve and shorter characteristic relaxation times, leading to overall "liquid-like" behavior while still maintaining phase segregation. The lack of side chain entanglements are observed in Booij−Palmen plots by the absence of relaxation plateaus in that regime. The overall "liquid-like" response and reduced viscosity of the dbBB were additionally compared to the entangled dbLin samples using plots of η^* vs G^*. Overall, the BBCPs behave similarly to the BB homopolymers according to SAOS characterizations. The microphase segregation seems to have very little effect on the behavior of $G'(\omega)$ and $G''(\omega)$, which is very different from the conventional LBCP. The rheological characterization confirms

DOI: 10.1021/acs.macromol.6b01471
Macromolecules 2017, 50, 396−405

the assumption that reduced chain entanglements can lead to fast ordering dynamics and milder thermal annealing conditions when compared to conventional LBCP materials. Shear-induced domain alignment was also observed at low strain amplitude within the LVR, which further highlights the unique behavior of BBCPs and the rich structure−property relationship. These findings emphasize the desirability and potential of the BBCP architectures for ease of processability in future applications.

■ ASSOCIATED CONTENT

Supporting Information

The Supporting Information is available free of charge on the ACS Publications website at DOI: 10.1021/acs.macromol.6b01471.

^{1}H NMR and GPC MALLS spectra of PS-*b*-PEO bottlebrush copolymers; TEM analysis of microphase-separated dbBBs; DSC measurements of dbBB materials; linear BCP dynamic response; 1D SAXS spectra of materials after rheological characterization; structural characterization of sheared linear BCP sample (PDF)

■ AUTHOR INFORMATION

Corresponding Authors

*E-mail: winter@ecs.umass.edu (H.H.W.).
*E-mail: watkins@polysci.umass.edu (J.J.W.).

Author Contributions

B.M.Y. and Y.G. contributed equally to the writing of the manuscript.

Notes

The authors declare no competing financial interest.

■ ACKNOWLEDGMENTS

This work is supported by the NSF Center for Hierarchical Manufacturing at the University of Massachusetts, Amherst (CMMI-1025020). The Materials Research Science and Engineering Center at University of Massachusetts Amherst supported facilities used in this work.

■ REFERENCES

(1) Xia, Y.; Kornfield, J. A.; Grubbs, R. H. Efficient Synthesis of Narrowly Dispersed Brush Polymers via. Living Ring-Opening Metathesis Polymerization of Macromonomers. *Macromolecules* **2009**, *42*, 3761−3766.

(2) Daniel, W. F. M.; Burdyńska, J.; Vatankhah-Varnoosfaderani, M.; Matyjaszewski, K.; Paturej, J.; Rubinstein, M.; Dobrynin, A. V.; Sheiko, S. S. Solvent-free, Supersoft and Superelastic Bottlebrush Melts and Networks. *Nat. Mater.* **2015**, *15*, 183−189.

(3) Hu, M.; Xia, Y.; McKenna, G. B.; Kornfield, J. A.; Grubbs, R. H. Linear Rheological Response of a series of Densely Branched Brush Polymers. *Macromolecules* **2011**, *44*, 6935−6943.

(4) Dalsin, S. J.; Hillmyer, M. A.; Bates, F. S. Molecular Weight Dependence of Zero-Shear Viscosity in Atactic Polypropylene Bottlebrush Polymers. *ACS Macro Lett.* **2014**, *3*, 423−427.

(5) Dalsin, S. J.; Hillmyer, M. A.; Bates, F. S. Linear Rheology of Polyolefin-Based Bottlebrush Polymers. *Macromolecules* **2015**, *48*, 4680−4691.

(6) López-Barrón, C. R.; Brant, P.; Eberle, A. P. R.; Crowther, D. J. Linear Rheology and Structure of Molecular Bottlebrushes with Short Side Chains. *J. Rheol.* **2015**, *59*, 865−883.

(7) Tsukahara, Y.; Namba, S. I.; Iwasa, J.; Nakano, Y.; Kaeriyama, K.; Takahashi, M. Bulk Properties of Poly(macromonomer)s of Increased Backbone and Branch Lengths. *Macromolecules* **2001**, *34*, 2624−2629.

(8) Verduzco, R.; Li, X.; Pesek, S. L.; Stein, G. E. Structure, Function, Self-assembly, and Applications of Bottlebrush Copolymers. *Chem. Soc. Rev.* **2015**, *44*, 2405−2420.

(9) Xia, Y.; Olsen, B. D.; Kornfield, J. A.; Grubbs, R. H. Efficient Synthesis of Narrowly Dispersed Brush Copolymers and Study of their Assemblies: The Importance of Side Chain Arrangement. *J. Am. Chem. Soc.* **2009**, *131*, 18525−18532.

(10) Bolton, J.; Rzayev, J. Synthesis and Melt Self-Assembly of PS−PMMA−PLA Triblock Bottlebrush Copolymers. *Macromolecules* **2014**, *47*, 2864−2874.

(11) Dalsin, S. J.; Rions-maehren, T. G.; Beam, M. D.; Bates, F. S.; Hillmyer, M. A.; Matsen, M. W. Bottlebrush Block Polymers: Quantitative Theory and Experiments. *ACS Nano* **2015**, *9*, 12233−12245.

(12) Rzayev, J. Synthesis of Polystyrene-polylactide Bottlebrush Block Copolymers and their Melt Self-assembly into Large Domain Nanostructures. *Macromolecules* **2009**, *42*, 2135−2141.

(13) Sveinbjornsson, B. R.; Weitekamp, R. A.; Miyake, G. M.; Xia, Y.; Atwater, H. A.; Grubbs, R. H. Rapid Self-assembly of Brush Block Copolymers to Photonic Crystals. *Proc. Natl. Acad. Sci. U. S. A.* **2012**, *109* (36), 14332−14336.

(14) Song, D.-P.; Li, C.; Colella, N. S.; Lu, X.; Lee, J.-H.; Watkins, J. J. Thermally Tunable Metallodielectric Photonic Crystals from the Self-Assembly of Brush Block Copolymers and Gold Nanoparticles. *Adv. Opt. Mater.* **2015**, *3*, 1169−1175.

(15) Song, D.-P.; Li, C.; Colella, N. S.; Xie, W.; Li, S.; Lu, X.; Gido, S.; Lee, J.-H.; Watkins, J. J. Large-Volume Self-Organization of Polymer/Nanoparticle Hybrids with Millimeter-Scale Grain Sizes Using Brush Block Copolymers. *J. Am. Chem. Soc.* **2015**, *137*, 12510−12513.

(16) Song, D.-P.; Li, C.; Li, W.; Watkins, J. J. Block Copolymer Nanocomposites with High Refractive Index Contrast for One-Step Photonics. *ACS Nano* **2016**, *10*, 1216−1223.

(17) Song, D.-P.; Lin, Y.; Gai, Y.; Colella, N. S.; Li, C.; Liu, X.-H.; Gido, S.; Watkins, J. J. Controlled Supramolecular Self-Assembly of Large Nanoparticles in Amphiphilic Brush Block Copolymers. *J. Am. Chem. Soc.* **2015**, *137*, 3771−3774.

(18) Choo, Y.; Mahajan, L. H.; Gopinadhan, M.; Ndaya, D.; Deshmukh, P.; Kasi, R. M.; Osuji, C. O. Phase Behavior of Polylactide-Based Liquid Crystalline Brushlike Block Copolymers. *Macromolecules* **2015**, *48*, 8315−8322.

(19) Deshmukh, P.; Gopinadhan, M.; Choo, Y.; Ahn, S. K.; Majewski, P. W.; Yoon, S. Y.; Kasi, R. M.; et al. Molecular Design of Liquid Crystalline Brush-like Block Copolymers for Magnetic Field Directed Self-assembly: A Platform for Functional Materials. *ACS Macro Lett.* **2014**, *3* (5), 462−466.

(20) Bates, F. S.; Fredrickson, G. H. Block Copolymers - Designer Soft Materials. *Phys. Today* **1999**, *52*, 32.

(21) Fredrickson, G. H.; Bates, F. S. Dynamics of Block Copolymers: Theory and Experiment. *Annu. Rev. Mater. Sci.* **1996**, *26*, 501−550.

(22) Matsen, M. W.; Bates, F. S. Unifying Weak- and Strong-Segregation Block Copolymer Theories. *Macromolecules* **1996**, *29*, 1091−1098.

(23) Chen, Z.-R.; Kornfield, J. A. Flow-induced Alignment of Lamellar Block Copolymer Melts. *Polymer* **1998**, *39* (19), 4679−4699.

(24) Chen, Z.-R.; Kornfield, J. A.; Smith, S. D.; Grothaus, J. T.; Satkowski, M. M. Pathways to Macroscale Order in Nanostructured Block Copolymers. *Science* **1997**, *277* (5330), 1248−1253.

(25) Darling, S. B. Directing the Self-assembly of Block Copolymers. *Prog. Polym. Sci.* **2007**, *32* (10), 1152−1204.

(26) Morrison, F.; Winter, H. H. The Effect of Unidirectional Shear on the Structure of Triblock Copolymers. I. Polystyrene-Polybutadiene-Polystyrene. *Macromolecules* **1989**, *22*, 3533−3540.

(27) Morrison, F.; Le Bourvellec, G.; Winter, H. H. Flow-Induced Structure and Rheology of a Triblock Copolymer. *J. Appl. Polym. Sci.* **1987**, *33*, 1585−1600.

(28) Koppi, K. A.; Tirrell, M.; Bates, F. S.; Almdal, K.; Colby, R. H. Lamellae Orientation in Dynamically Sheared Diblock Copolymer Melts. *J. Phys. II* **1992**, *2*, 1941−1959.

DOI: 10.1021/acs.macromol.6b01471
Macromolecules 2017, 50, 396−405

(29) Winey, K.; Patel, S. S.; Larson, R. G. Interdependence of Shear Deformations and Block Copolymer Morphology. *Macromolecules* **1993**, *26*, 2542−2549.
(30) Riise, B. L.; Fredrickson, G. H.; Larson, R. G.; Pearson, D. S. Rheology and Shear-Induced Alignment of Lamellar Diblock and Triblock Copolymers. *Macromolecules* **1995**, *28* (23), 7653−7659.
(31) Vigild, M. E.; Chu, C.; Sugiyama, M.; Chaffin, K. A.; Bates, F. S. Influence of Shear on the Alignment of a Lamellae-Forming Pentablock Copolymer. *Macromolecules* **2001**, *34*, 951−964.
(32) Pakula, T.; Zhang, Y.; Matyjaszewski, K.; Lee, H.-I.; Boerner, H.; Qin, S.; Berry, G. C. Molecular Brushes as Super-soft Elastomers. *Polymer* **2006**, *47*, 7198−7206.
(33) Lin, Y.; Wang, Y.; Zheng, J.; Yao, K.; Tan, H.; Wang, Y.; Tang, T.; Xu, D. Nanostructure and Linear Rheological Response of Comb-like Copolymer PSVS- *g* -PE Melts: Influences of Branching Densities and Branching Chain Length. *Macromolecules* **2015**, *48*, 7640−7648.
(34) De La Fuente, J. L.; Fernandez-Garcia, M.; Cerrada, M. L.; Spiess, H. W.; Wilhelm, M. Small-angle X-ray Scattering and Linear Melt Rheology of poly(tert-butyl acrylate-g-styrene) Graft Copolymers. *Polymer* **2006**, *47* (5), 1487−1495.
(35) De La Fuente, J. L.; Wilhelm, M.; Spiess, H. W.; Madruga, E. L.; Fernandez-Garcia, M.; Cerrada, M. L. Thermal, Morphological and Rheological Characterization of poly(acrylic acid-g-styrene) Amphiphilic Graft Copolymers. *Polymer* **2005**, *46* (13), 4544−4553.
(36) Wang, L.; Yang, H.; Tan, H.; Yao, K.; Gong, J.; Wan, D.; Tang, T. Synthesis and Structure-property Relationships of Polypropylene-g-Polystyrene and Polypropylene-g-Poly(n-butyl acrylate) Graft Copolymers with Well-defined Molecular Structures. *Polymer* **2013**, *54* (14), 3641−3653.
(37) Namba, S.; Tsukahara, Y.; Kaeriyama, K.; Okamoto, K.; Takahashi, M. Bulk Properties of Multibranched Polystyrenes from Polystyrene Macromonomers: Rheological Behavior I. *Polymer* **2000**, *41*, 5165−5171.
(38) Bates, C. M.; Chang, A. B.; Schulze, M. W.; Momcilovic, N.; Jones, S. C.; Grubbs, R. H. Brush Polymer Ion Gels. *J. Polym. Sci., Part B: Polym. Phys.* **2016**, *54*, 292−300.
(39) Bates, C. M.; Chang, A. B.; Schulze, M. W.; Momcilovic, N.; Jones, S. C.; Grubbs, R. H. ABA Triblock Brush Polymers: Synthesis, Self-Assembly, Conductivity and Rheological Properties. *Macromolecules* **2015**, *48*, 4967−4973.
(40) Gai, Y.; Song, D.-P.; Yavitt, B. M.; Watkins, J. J. Polystyrene-*block*-Poly (ethylene oxide) Bottlebrush Block Copolymer Morphology Transitions: Influence of Side Chain Length and Volume Fraction. *Macromolecules* **2016**, submitted.
(41) Winter, H. H.; Mours, M. The Cyber Infrastructure Initiative for Rheology. *Rheol. Acta* **2006**, *45* (4), 331−338.
(42) Williams, M. L.; Landel, R. F.; Ferry, J. D. The Temperature Dependence of Relaxation Mechanisms in Amorphous Polymers and Other Glass-forming Liquids1. *J. Am. Chem. Soc.* **1955**, *77* (12), 3701−3707.
(43) van Gurp, M.; Palmen, J. Time-temperature Superposition for Polymeric Blends. *J. Rheol Bull.* **1998**, *65*, 5−8.
(44) Booij, H. C.; Palmen, J. In *Theoretical and Applied Rheology*, 1st ed.; Moldenaers, P., Keunings, R., Eds.; Elsevier Science: Brussels, 1992; p 321.
(45) Booij, H. C.; Palmen, J. Some aspects of Linear and Nonlinear Viscoelastic Behavior of Polymer Melts in Shear. *Rheol. Acta* **1982**, *21*, 376−387.
(46) Han, C. D.; Kim, J. K. On the Use of Time-Temperature Superposition in Multicomponent/multiphase Polymer Systems. *Polymer* **1993**, *34* (12), 2533−2539.
(47) Trinkle, S.; Friedrich, C. Van Gurp-Palmen-plot: A Way to Characterize Polydispersity of Linear Polymers. *Rheol. Acta* **2001**, *40*, 322−328.
(48) Baumgaertel, M.; Winter, H. H. Determination of Discrete Relaxation and Retardation Time Spectra from Dynamic Mechanical Data. *Rheol. Acta* **1989**, *28*, 511−519.
(49) Colby, R. H. In *Encyclopedia of Materials: Science and Technology*, 2nd ed.; Buschow, K. H. J., Cahn, R. W., Flemings, M. C., Ilschner, B., Kramer, E. J., Eds.; Elsevier Science: Oxford, 2001; p 727.
(50) Scott, D. B.; Waddon, A. J.; Lin, Y. G.; Karasz, F. E.; Winter, H. H. Shear-induced Orientation Transitions in Triblock Copolymer Styrene-butadiene-styrene with Cylindrical Domain Morphology. *Macromolecules* **1992**, *25* (16), 4175−4181.
(51) Winter, H. H. Three Views for Viscoelasticity of Cox-Merz Materials. *Rheol. Acta* **2009**, *48*, 909−916, DOI: 10.1007/s00397-008-0329-5.

DOI: 10.1021/acs.macromol.6b01471
Macromolecules 2017, 50, 396−405